Single-layer oxychloride superconductor $Ca_{2-x}CuO_2Cl_2$ with *A*-site cation deficiency

I. Yamada,[1,*] A. A. Belik,[2,†] M. Azuma,[1,2] S. Harjo,[3,‡] T. Kamiyama,[3] Y. Shimakawa,[1] and M. Takano[1]
[1]*Institute for Chemical Research, Kyoto University, Uji, Kyoto 611-0011, Japan*
[2]*PRESTO, Japan Science and Technology Corporation, Kawaguchi, Saitama 332-0012, Japan*
[3]*Institute of Materials Structure Science, High Energy Accelerator Research Organization, Tsukuba, Ibaraki 305-0801, Japan*
(Received 9 June 2005; revised manuscript received 9 August 2005; published 7 December 2005)

An oxychloride superconductor $Ca_{2-x}CuO_2Cl_2$ with a single CuO_2 plane in the unit cell was prepared without cation substitution using high-pressure synthesis. The highest T_C was 38 K, 10 K higher than that of $Ca_{2-x}Na_xCuO_2Cl_2$. Structure analysis based on synchrotron x-ray and neutron powder diffractions revealed that the Ca deficiency was the origin of the hole carrier. This compound has two structural features as compared to $Ca_{2-x}Na_xCuO_2Cl_2$; fewer defects and a shorter Cu-Cl bond length. Postannealing at 773 K led to a further increase of the T_C to 43 K. This superconductor with a flat CuO_2 plane might form the basis for future discussions about the factors that determine the T_C of single-layer cuprates.

DOI: 10.1103/PhysRevB.72.224503 PACS number(s): 74.72.Jt, 74.62.Dh, 61.12.Ld

I. INTRODUCTION

Superconductivity in copper oxides occurs when an adequate number of hole or electron carriers are introduced into an antiferromagnetic insulator with CuO_2 planes. La_2CuO_4 becomes superconducting when the La^{3+} ions are partially substituted by divalent alkaline earth ions like Sr^{2+}. Hole doping can, however, be done in another way. It is well-established that the injection of excess oxygen into interstitial sites works as well.[1] In this paper we will show that in the case of $Ca_2CuO_2Cl_2$ deficiency of the counter cation, Ca^{2+}, also works. Mentioning a related known example, the metallic ferromagnet generally formulated as $LaMnO_{3+\delta}$ contains, in fact, cation deficiencies as $La_{1-\alpha}Mn_{1-\beta}O_3$.[2]

Copper oxychloride $Ca_2CuO_2Cl_2$ has a single CuO_2 plane, the same as La_2CuO_4. Figure 1 shows the crystal structure of $Ca_2CuO_2Cl_2$ in tetragonal unit cell of $a=3.87$ Å and $c=15.05$ Å.[3] This can be derived from La_2CuO_4 by replacing La with Ca and apical oxygen with chlorine, and is antiferromagnetic insulator with $T_N=250$ K,[4] as other parent compounds of copper oxide superconductors. In spite of the structural features, $Ca_2CuO_2Cl_2$ was known as a candidate parent compound of superconductor with a flat CuO_2 plane, i.e., it was impossible to introduce mobile carriers. Hole doping by substituting Na for Ca to make this compound superconducting was accomplished using high-pressure (HP) synthesis at 6 GPa.[5] Samples in the left half of the bell-shaped superconducting phase diagram have been obtained so far.[6] $Ca_{2-x}Na_xCuO_2Cl_2$ has the highest $T_C=28$ K at $x=0.20$. The ease of sample preparation with a lightly hole-doped composition, an absence of structural changes at low temperature, an absence of structural modulation, and excellent single crystal sample cleavage[7] are ideal for surface sensitive measurements. Investigations into this compound's electronic state using angle-resolved photoemission spectroscopy[8–10] and scanning tunneling microscopy/spectroscopy[11,12] are attracting great attention.

Recently, we discovered a $Ca_2CuO_2Cl_2$-based superconductor with the highest T_C of 38 K using HP synthesis without Na substitution.[13] Two possibilities were suggested for the hole carrier origin; the presence of a calcium deficiency and presence of interstitial chlorine. However, no conclusions were reached at that time. Here we describe the results of the structural determination of this superconductor. Structural analyses based on synchrotron x-ray and neutron powder diffraction clearly show that Ca deficiency exists in the superconducting samples.

II. EXPERIMENT

A precursor $Ca_2CuO_2Cl_2$ from $CaCO_3$ (99.99%), CuO (99.99%), and $CaCl_2$ (99.99%) was prepared by a solid-state reaction in a N_2 flow at ambient pressure. The resulting $Ca_2CuO_2Cl_2$ was mixed with $CaCl_2$ (99.99%), CuO (99.99%), and $Ca(ClO_4)_2$ (99%) to form $Ca_{2-x}CuO_2Cl_2$ and $Ca_2CuO_2Cl_{2+y}$. The former is a calcium deficient composition, while the latter contains excess chlorine. The $Ca(ClO_4)_2$ was dried in air at 370 °C for 12 h in advance. A gold capsule

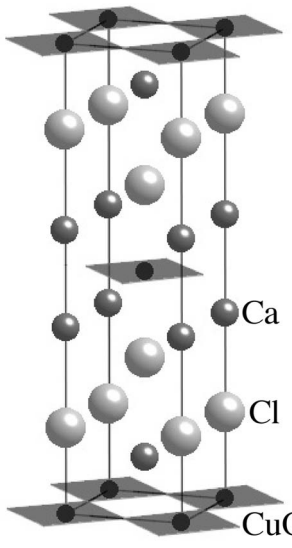

FIG. 1. Crystal structure of the oxychloride $Ca_2CuO_2Cl_2$. The black, small and large gray spheres correspond to the Cu, Ca, and Cl ions, respectively. Oxygen appears in the corners of the squares.

charged with the earlier mixture was placed in a high-pressure cell and compressed to 6 GPa in a cubic anvil type high-pressure apparatus. The sample was then heated at 1273 K for 30 min and quenched to room temperature before releasing the pressure. The weighting, the mixing, and the capsule filling procedures were performed in an Ar filled drybox to avoid influence of moisture. Powder x-ray diffraction (XRD) patterns with Cu $K\alpha$ radiation were taken with a Rigaku RINT 2500 diffractometer to identify the phases. Synchrotron x-ray diffraction (SXRD) patterns were collected for the samples with various starting compositions at room temperature with a large Debye-Scherrer camera[14] installed at the beam line BL02B2 of SPring-8 with $\lambda = 0.775\,976$ Å ($x_n = 0$, 0.1, and 0.2 samples) and 0.775 640 Å ($x_n = 0.15$ sample). The powder sample's granularity was homogenized to 2–3 μm in diameter using a precipitation method in hexane.[15,16] Neutron powder diffraction (NPD) data were taken on the 2 g m of as-synthesized pellets of the sample with the highest T_C, using the Vega[17] time-of-flight neutron diffractometer at KENS. The structural parameters were refined by Rietveld analyses using RIETAN-2000 (Ref. 18) and RIETAN-TN (Ref. 19) software. Magnetic susceptibilities were measured on cooling using a Quantum Design superconducting quantum interference device MPMS in an external field of 10 Oe.

III. RESULTS AND DISCUSSION

We observed superconductivity with the highest T_C of 38 K for both sets of samples, $Ca_{2-x}CuO_2Cl_2$ and $Ca_2CuO_2Cl_{2+y}$ in nominal compositions of $x_n \sim 0.2$ and $y_n \sim 0.4$, respectively. No peaks attributed to the double or triple layer oxychloride phase were found in the XRD patterns. The a axis shrunk while the c axis expanded as x_n and y_n increased, and the relationship between the lattice parameters and T_C were essentially the same for both series. It is reasonable to assume that the same superconducting phase was obtained from the initial two compositions. However, a considerable amount of $CaCl_2 \cdot 2H_2O$ impurities were found only in the sample prepared from $Ca_2CuO_2Cl_{2+y}$. This suggests that the superconducting phase was $Ca_{2-x}CuO_2Cl_2$ and the remaining Ca and Cl formed $CaCl_2$ and then absorbed the moisture from the air. Therefore, SXRD and NPD measurements were performed on $Ca_{2-x}CuO_2Cl_2$ samples to confirm the calcium deficiency.

Figure 2 shows the SXRD and NPD patterns for the sample with the nominal $Ca_{1.8}CuO_2Cl_2$ ($x_n = 0.2$) composition with $T_C = 38$ K. Because we could not observe any reflection indicating a superlattice, the structure refinements were performed based on the $I4/mmm$ space group (No. 139), the same as that of $Ca_2CuO_2Cl_2$. A small amount of CuO (1.97 wt %) was found as an impurity phase only in NPD data. In contrast, CaCl(OH) impurity (5 wt %, typically) was found in SXRD data. The absence of the CuO peaks in SXRD patterns can be attributed to its higher density compared with Ca containing phases because heavy particles are separated during the precipitation process. CaCl(OH) formed probably because of the reaction between water contaminated in hexane and $CaCl_2$ formed as a result

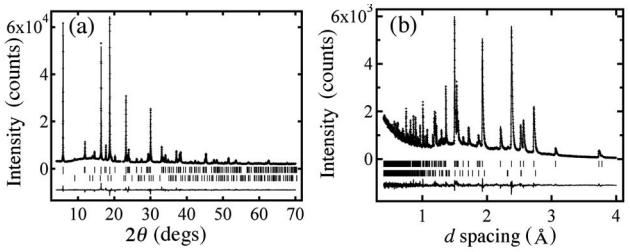

FIG. 2. (a) Synchrotron x-ray and (b) neutron powder diffraction patterns for the sample with the nominal composition of $Ca_{1.8}CuO_2Cl_2$ ($x_n = 0.20$), taken at room temperature. Dots and lines show the observed and calculated patterns. The difference between the observed and fitted patterns is displayed at the bottom of the figures. The upper and lower vertical marks correspond to the diffraction positions of $Ca_{2-x}CuO_2Cl_2$ and impurities of CaCl(OH) (SXRD) and CuO (NPD), respectively.

of partial decomposition of the particle surface after the heavy grinding. We have confirmed that T_C and the lattice constants did not change before and after the precipitation process, so this procedure did not affect the sample composition. Our analyses of the SXRD data are still reliable since the results are in good agreement with that of NPD data as described below. The sample used for NPD measurement was not crushed as synthesized pellets. Furthermore, neutron is sensitive for light elements such as O and Cl. On the other hand, NPD requires a large amount of sample which is hard to prepare by the HP synthesis. Therefore, we collected the NPD data for only one composition. Both the calcium deficiency ($Ca_{2-x}CuO_2Cl_2$) and the interstitial chlorine ($Ca_2CuO_2Cl_{2+x}$, excess chlorine ions were placed at 1/2, 0, 1/4 between the two Cl layers, the same as $Sr_2CuO_2F_{2+\delta}$)[20] models were examined during the early refinement stage of the SXRD and NPD data. The occupancy of the interstitial chlorine site in the interstitial chlorine model was zero within the standard deviation, while the calcium site occupancy in the calcium deficiency model decreased from 1. We also investigated the possibility of a partial replacement of oxygen with chlorine, but found no trace. Therefore the Cu, O, and Cl occupancies were fixed to 1 and only the calcium occupancy was refined, as well as the lattice constants, the Ca and Cl positions, and the thermal displacement parameters during the final refinement stage. The good agreement of the calcium occupancies in both the SXRD and NPD results and satisfactory low R factors (reliable factors for the overall fittings and for the individual phases are typical values for SXRD and NPD) and the goodness of fit S (~ 1.4) confirmed the validity of our analysis. We later analyzed the SXRD data for other samples assuming the presence of a Ca deficiency. The refined structural parameters are summarized in Table I. It is known that the parameters of occupancy (g) and thermal displacement parameter (B) are strongly correlated to each other. To estimate the influence of the latter parameter on the former, we fixed the B parameter of Ca at 0.79 and refined the g value for all the SXRD data. This value of 0.79 was chosen because it led to the same g value of 0.954 as determined by ND for the $x_n = 0.2$ sample. The resulting g values were 1.0038(9), 0.981(1), 0.976(1), and 0.954(2) for the $x_n = 0$, 0.1, 0.15, and 0.2 samples, respectively. Since the differ-

TABLE I. Refined structural parameters for $Ca_2CuO_2Cl_2$, $Ca_{2-x}CuO_2Cl_2$. The data were analyzed based on the spage group $I4/mmm$ with Ca, Cu, O, and Cl placed at (0, 0, z), (0,0,0), (0,1/2,0), and (0,0,z), respectively.

			$Ca_2CuO_2Cl_2$	$Ca_{1.9}CuO_2Cl_2$	$Ca_{1.85}CuO_2Cl_2$	$Ca_{1.8}CuO_2Cl_2$		$Ca_{1.8}CuO_2Cl_2$ (NPD)
Ca	4*e*	*g*	0.996(1)	0.976(2)	0.963(2)	0.954(2)	*g*	0.954(4)
		z	0.39567(3)	0.39477(5)	0.39405(7)	0.39419(6)	*z*	0.3950(1)
		B	0.66(1)	0.67(2)	0.50(2)	0.79(2)	U_{11}	0.0048(5)
							U_{33}	0.012(1)
Cu	2*a*	*g*	1[a]	1[a]	1[a]	1[a]	*g*	1[a]
		B	0.448(9)	0.54(1)	0.39(2)	0.53(2)	U_{11}	0.00027(5)
							U_{33}	0.00416(5)
O	4*c*	*g*	1[a]	1[a]	1[a]	1[a]	*g*	1[a]
		B	0.78(2)	0.90(5)	0.67(6)	0.71(5)	U_{11}	0.031(4)[b]
							U_{22}	0.031(4)[b]
							U_{33}	0.074(9)
Cl	4*e*	*g*	1[a]	1[a]	1[a]	1[a]	*g*	1[a]
		z	0.18230(3)	0.18117(6)	0.18077(7)	0.18086(6)	*z*	0.18131(7)
		B	0.87(1)	0.84(2)	0.72(2)	0.84(2)	U_{11}	0.0077(3)
							U_{33}	0.0060(6)
a		3.86735(2)	3.85637(8)	3.8549(1)	3.85214(5)	*a*	3.85155(6)	
c		15.0412(1)	15.0984(3)	15.1132(5)	15.1224(2)	*c*	15.1125(3)	
R_{wp}^c		2.07	2.32	2.51	2.52	R_{wp}^c	4.20	
R_I^c		1.96	2.25	1.56	1.33	R_I^c	2.66	
S^c		1.26	1.44	1.05	1.44	S^c	1.54	

[a]The following constraints were applied to the synchrotron x-ray diffraction and neutron data: $g(\mathrm{Cu})=g(\mathrm{O})=g(\mathrm{Cl})=1$.
[b]The following constraint was applied to the neutron diffraction data: $U_{22}(\mathrm{O})=U_{11}(\mathrm{O})$.
[c]$R_{wp}=\{\Sigma_i w_i\{y_i(\mathrm{obs.})-y_i(\mathrm{calc.})\}/\Sigma_i w_i[y_i(\mathrm{obs.})]^2\}^{1/2}$, $R_I=\Sigma_K|I_K(\mathrm{obs.})-I_K(\mathrm{calc.})|/\Sigma_K|I_K(\mathrm{obs.})|$, $S=[\Sigma_i w_i\{y_i(\mathrm{obs.})-y_i(\mathrm{calc.})\}/N-P]^{1/2}$, where y_i(obs./calc.) is the observed/calculated intensity at the ith step, w_i is $1/y_i$, I_K(obs./calc.) is the observed/calculated intensity assigned to the Kth Bragg reflection, N is the number of observations, and P is the number of parameters adjusted.

ences are small, we employ the g values with B's refined in the following discussion. Figure 3 shows the lattice parameter changes as functions of the refined x_r values. The a axis shrunk as the Ca deficiency increased, indicating that the hole carrier was introduced in the CuO_2 plane while the c axis expanded. These changes were similar to those of $Ca_{2-x}Na_xCuO_2Cl_2$ and other p-type superconductors. As shown in Fig. 4, there was a linear relationship between the nominal and the refined Ca deficiency, $x_r=0.473\,x_n$. It should be noted that this reduced carrier concentration from the nominal composition was also observed in $Ca_{2-x}Na_xCuO_2Cl_2$. Inclusion of the impurity phases such as CuO could be the reason for these discrepancies. In fact, the mole ratio of Ca and Cu estimated from the NPD refinement was Ca:Cu=1.79(7):1, in good agreement with the nominal composition $Ca_{1.8}CuO_2Cl_2$ of the starting mixture.

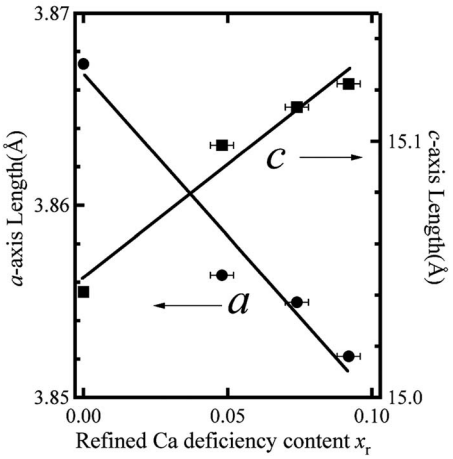

FIG. 3. The lattice parameter changes as functions of the refined x_r values. The lines are guides to the eye.

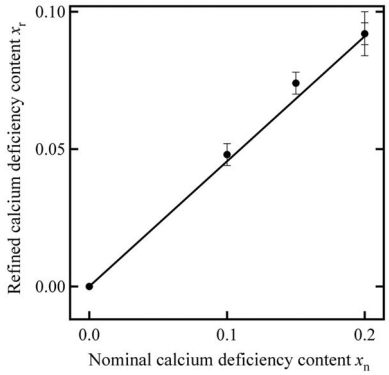

FIG. 4. The refined calcium deficiency concentration x_r as a function of the nominal composition x_n in $Ca_{2-x}CuO_2Cl_2$. The line corresponds to $x_r=0.473x_n$ obtained using the least-squares method.

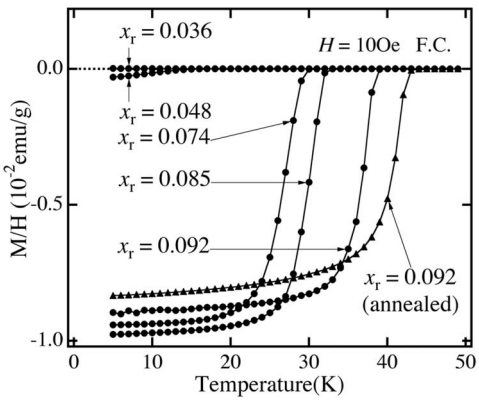

FIG. 5. Temperature dependences of the magnetic susceptibility of $Ca_{2-x}CuO_2Cl_2$ (x_r=0.036, 0.048, 0.074, 0.085, and 0.092) measured on cooling in an external field of 10 Oe. The x_r values of 0.048, 0.074, and 0.092 were determined from the structure refinements. We estimated 0.036 and 0.085 from the nominal composition using the equation $x_r=0.473\ x_n$ given in the discussion.

Figure 5 shows the temperature dependences of the magnetic susceptibility for samples with various Ca deficiencies. The parent compound, $Ca_2CuO_2Cl_2$, did not show any trace of superconductivity, while the $x_r=0.048$ sample showed a weak diamagnetism below 15 K. Both the T_C and the volume fraction increased as x_r increased, and the $x_r=0.092$ sample showed the highest T_C of 38 K. The large diamagnetic susceptibility of -9×10^{-2} emu/g corresponded to the Meissner volume fraction of about 50%. The T_C for $Ca_{2-x}CuO_2Cl_2$ is plotted in Fig. 6, along with that of $Ca_{2-x}Na_xCuO_2Cl_2$,[6] as functions of the calculated carrier number per Cu. Both showed a similar carrier number dependence, in which T_C appeared at $0.07<n_C<0.1$ and increased monotonically. However, the former showed a higher T_C within the entire composition range.

The reason for the T_C increase is not clear at this stage of the study, but we suggest two possibilities based on the comparison with $Ca_{2-x}Na_xCuO_2Cl_2$. One possibility is that the

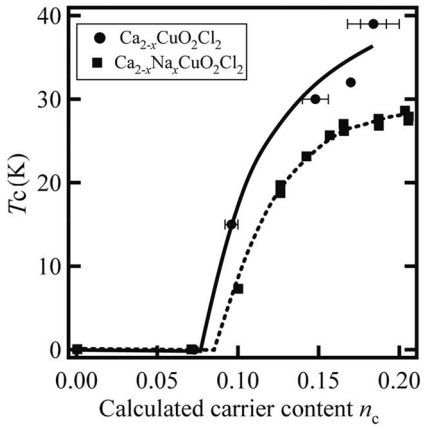

FIG. 6. Variations of T_C for $Ca_{2-x}CuO_2Cl_2$ (circles) and $Ca_{2-x}Na_xCuO_2Cl_2$ (squares) as functions of the hole concentration per Cu ions, n_C (twice the x value for $Ca_{2-x}CuO_2Cl_2$ and the same as the x values for $Ca_{2-x}Na_xCuO_2Cl_2$, respectively). The curves are for reference purposes.

TABLE II. Selected bond and c axis lengths (in angstroms) for $Ca_2CuO_2Cl_2$, $Ca_{1.952}CuO_2Cl_2$, and $Ca_{1.90}Na_{0.10}CuO_2Cl_2$.

	$Ca_2CuO_2Cl_2$	$Ca_{1.952}CuO_2Cl_2$	$Ca_{1.90}Na_{0.10}CuO_2Cl_2$
Cu-O (=a/2)	1.93368(1)	1.92819(4)	1.9248(1)
Cu-Cl	2.7420(5)	2.7347(1)	2.7615(3)
c	15.0412(1)	15.0984(3)	15.1729(5)

structural defects created by the cation substitution or deficiency reduce the T_C. The number of the structural defects is half of that of $Ca_{2-x}Na_xCuO_2Cl_2$ with the same hole concentration. This is because one Ca vacancy contains two holes, while replacing a Ca ion with a Na ion creates only one hole. The influences of the ionic size differences of two elements occupying the A sites were investigated for La-214 (Ref. 21) and Bi-2201 systems.[22] In both compounds, a larger ionic radius mismatch results in lower T_C. In our system, the size difference between Ca^{2+} and the vacancy is much larger than that of Ca^{2+} and Na^+. However, the number of defects, another factor reducing the T_C, is half of that of $Ca_{2-x}Na_xCuO_2Cl_2$ as described above. Considering these two points, the influence of the defect concentration exceeds that of the size mismatch in the present system.

Another possibility is that the position of the chlorine ion at the CuO_4Cl_2 octahedron apex governs the T_C. The Cu-Cl bond length of $Ca_{2-x}CuO_2Cl_2$ was 1% shorter than that of $Ca_{2-x}Na_xCuO_2Cl_2$,[23] as shown in Table II. The $Ca_{1.952}CuO_2Cl_2$ Cu-Cl bond is even shorter than that of the parent compound $Ca_2CuO_2Cl_2$, although the c axis expanded with the Ca deficiency. In the $Ca_2CuO_2Cl_2$ crystal structure, large chlorine ions are not in the Ca plane. Introducing a Ca deficiency relaxes the spatial restrictions, so chlorine ions can move closer to the CuO_2 plane. For p-type high-T_C superconductors in underdoped regions, pressure applications in the c axis (perpendicular to the CuO_2 plane) increase T_C because the holes localized at the apical oxygens are transferred to the CuO_2 plane.[24,25] The exception is the La-214 system where application of uniaxial pressure stabilizes the stripe order and thus suppresses T_C.[26] A T_C measurement under uniaxial pressure on single crystal $Ca_{2-x}Na_xCuO_2Cl_2$ clarifies the influence of the Cu-Cl length on T_C.

It should also be noted that annealing the $x_r=0.092$ sample at 773 K in a quartz vacuum tube for 12 h led to a further increase in T_C to 43 K, as plotted in Fig. 5. Because the same T_C was obtained for the sample annealed in an oxygen flow at 773 K for 12 h, we know the carrier concentration change caused by introducing or removing excess oxygen does not cause the T_C increase. One possible explanation is that the microscopic strain in the crystal structure caused during the pressure release was relaxed during the annealing procedure. Another possibility is that the Ca vacancies ordered during annealing. Such ordering reduces the inhomogeneities and randomness in the system, so is expected to enhance T_C as discussed in Ref. 22. No superlattice peaks were found in the SXRD pattern for the annealed

sample, but this alone is not enough to eliminate the possibility of ordering. Unfortunately, we were unable to complete the electron diffraction study essential for such ordered structures because of the high reactivity of the sample containing moisture.

In conclusion, we fabricated a single-layer oxychloride superconductor with $T_C = 38$ K using high-pressure synthesis. Structure analyses based on synchrotron x-ray and neutron powder diffractions clearly showed that the Ca deficiency was the origin of the hole carrier. The T_C further increased to 43 K after post annealing at 773 K. This superconductor with a flat CuO_2 plane might be a model compound for discussions about the factors determining the T_C of single-layer cuprates.

ACKNOWLEDGMENTS

The synchrotron radiation experiments were performed at the SPring-8 with the approval of the Japan Synchrotron Radiation Research Institute. We would like to express our thanks to the Ministry of Education, Culture, Sports, Science and Technology, Japan, for Grants-in-Aid Nos. 13440111, 14204070, and 12CE2005 for COE Research on Elements Science, and for 21COE on the Kyoto Alliance for Chemistry.

*Electronic address: ikuya@msk.kuicr.kyoto-u.ac.jp
†Present address: International Center for Young Scientists, National Institute for Materials Science, Namiki 1-1, Tsukuba, Ibaraki, 305-0044, Japan.
‡Present address: Neutron Science Research Center, Japan Atomic Energy Research Institute, Tokai, Ibaraki 319-1195, Japan.

[1] J. D. Jorgensen, B. Dabrowski, S. Pei, D. G. Hinks, and L. Soderholm, Phys. Rev. B **38**, 11337 (1988).
[2] J. A. M. Van Roosmalen, E. H. P. Cordfunke, and R. B. Helmholdt, J. Solid State Chem. **110**, 100 (1994).
[3] H. Müller-Buschbaum, Angew. Chem., Int. Ed. Engl. **16**, 674 (1977).
[4] D. Vaknin, L. L. Miller, and J. L. Zaretsky, Phys. Rev. B **56**, 8351 (1997).
[5] Z. Hiroi, N. Kobayashi, and M. Takano, Nature **371**, 139 (1994).
[6] Z. Hiroi, N. Kobayashi, and M. Takano, Physica C **266**, 191 (1996).
[7] Y. Kohsaka, M. Azuma, I. Yamada, T. Sasagawa, T. Hanaguri, M. Takano, and H. Takagi, J. Am. Chem. Soc. **124**, 12275 (2002).
[8] Y. Kohsaka, T. Sasagawa, F. Ronning, T. Yoshida, C. Kim, T. Hanaguri, M. Azuma, M. Takano, Z. X. Shen, and H. Takagi, J. Phys. Soc. Jpn. **72**, 1018 (2003).
[9] K. M. Shen, F. Ronning, D. H. Lu, W. S. Lee, N. J. C. Ingle, W. Meevasana, F. Baumberger, A. Damascelli, N. P. Armitage, L. L. Miller, Y. Kohsaka, M. Azuma, M. Takano, H. Takagi, and Z.-X. Shen, Phys. Rev. Lett. **93**, 267002 (2004)
[10] K. M. Shen, F. Ronning, D. H. Lu, F. Baumberger, N. J. C. Ingle, W. S. Lee, W. Meevasana, Y. Kohsaka, M. Azuma, M. Takano, H. Takagi, and Z.-X. Shen, Science **307**, 901 (2005).
[11] Y. Kohsaka, K. Iwaya, S. Satow, T. Hanaguri, M. Azuma, M. Takano, and H. Takagi, Phys. Rev. Lett. **93**, 097004 (2004)
[12] T. Hanaguri, C. Lupien, Y. Kohsaka, D.-H. Lee, M. Azuma, M. Takano, H. Takagi, and J. C. Davis, Nature **430**, 1001 (2004).
[13] I. Yamada, M. Azuma, and M. Takano, Physica C **412-414**, 27 (2004).
[14] E. Nishibori, M. Takata, K. Kato, M. Sakata, Y. Kubota, S. Aoyagi, Y. Kuroiwa, M. Yamakata, and N. Ikeda, Nucl. Instrum. Methods Phys. Res. A **467-468**, 1045 (2001).
[15] M. Takata, E. Nishibori, K. Kato, M. Sakata, and Y. Moritomo, J. Phys. Soc. Jpn. **68** 2190 (1999).
[16] S. Ishiwata, M. Azuma, M. Takano, E. Nishibori, M. Takata, M. Sakata, and K. Kato, J. Mater. Chem. **12**, 3733 (2002).
[17] T. Kamiyama, K. Oikawa, N. Tsuchiya, M Osawa, H. Asano, N. Watanabe, M. Furusaka, S. Satoh, I. Fujikawa, T. Ishigaki, and F. Izumi, Physica B **213-214**, 875 (1995).
[18] F. Izumi and T. Ikeda, Mater. Sci. Forum **198**, 321 (2000).
[19] T. Ohta, F. Izumi, K. Oikawa, and T. Kamiyama, Physica B **234-236**, 1093 (1997).
[20] M. Al-Mamouri, P. P. Edwards, C. Greaves, and M. Slaski, Nature **369**, 382 (1994).
[21] J. P. Attfield, A. L. Kharlanov, and J. A. McAllister, Nature **394**, 157 (1998)
[22] H. Eisaki, N. Kaneko, D. L. Feng, A. Damascelli, P. K. Mang, K. M. Shen, Z.-X. Shen, and M. Greven, Phys. Rev. B **69**, 064512 (2004).
[23] D. N. Argyriou, J. D. Jorgensen, R. L. Hitterman, Z. Hiroi, N. Kobayashi, and M. Takano, Phys. Rev. B **51**, 8434 (1995).
[24] C. Meingast, J. Karpinski, E. Jilek, and E. Kaldis, Physica C **209**, 591 (1993).
[25] L. Gao, Y. Y. Xue, F. Chen, Q. Xiong, R. L. Meng, D. Ramirez, C. W. Chu, J. H. Eggert, and H. K. Mao, Phys. Rev. B **50**, 4260 (1994).
[26] F. Nakamura, M. Kodama, S. Sakita, Y. Maeno, and T. Fujita, Phys. Rev. B **54**, 10061 (1996).